1076 *Macromolecules* **2010**, *43*, 1076–1082
DOI: 10.1021/ma901267s

Macromolecules
ARTICLE

Double Glass Transitions and Interfacial Immobilized Layer in in-Situ-Synthesized Poly(vinyl alcohol)/Silica Nanocomposites

Lin Chen,[†] Kang Zheng,[†] Xingyou Tian,[†] Kun Hu,[†] Ruoxi Wang,[†] Chen Liu,[†] Yong Li,[‡] and Ping Cui*,[†,‡]

[†]*Key Laboratory of Materials Physics, Institute of Solid State Physics, Chinese Academy of Sciences, P.O. Box 1129, Hefei 230031, P. R. China and* [‡]*Ningbo Institute of Material Technology and Engineering, Chinese Academy of Sciences, Ningbo 315201, P. R. China*

Received June 12, 2009; Revised Manuscript Received December 11, 2009

ABSTRACT: The results of dynamic mechanical analysis (DMA) revealed that there were double tan δ peaks in the poly(vinyl alcohol)(PVA)/silica nanocomposite samples at low frequencies. The two relaxations attribute to glass transition for PVA matrix and motions of segments for PVA chains confined by the surface of silica nanoparticles, respectively. The thickness of the interfacial immobilized layer was calculated, and schematic models were founded, which can well interpret the results. The changes of the two relaxations with various silica contents at different frequencies are discussed. It is considered that most of the interfacial PVA chains probably span the two layers. The peak position of the first relaxation moves to high temperature with the increase of frequency for strain lag of the sample whereas the second one shifts to low temperature for the "drag effect" between the intrinsic and interfacial segments of the spanned PVA chains.

Introduction

In recent years, polymer/inorganic nanocomposites have drawn more attention for their fabulous characteristics and potentially commercial applications.[1−3] The properties of the composites are probably dominated or strongly influenced by the interfacial effects between the polymer and inorganic nanoparticles.

Size and confinement effects at the nanometer size scale on the glass transition temperature and the dynamics of polymer chains at the interface with particles have been well reviewed by Alcoutlabi and McKenna[4] and by Robertson and Roland,[5] respectively. It was concluded that surface effects existed on the observed changes in the glass transition or its associated dynamics. The dynamics of interfacial molecules have already been investigated by various techniques.[4−10] The phenomena that two glass transitions for small molecular weight glass-formers[4,11,12] in nanometer scale pores were observed and interpreted by a two-layer model: a bulklike core layer in the pore volume and an interfacial layer close to the pore wall under nanoconfinement. A three-layer model[13] has also been proposed to interpret the dynamics of H-bonded liquids confined in nanopores. For polymer nanocomposites, the glass transition temperature T_g has been reported to increase,[14,15] decrease,[16] or remain unchanged[17,18] in the previous researches for various confinement effects or surface interactions. Moreover, the model proposed by Berriot et al.[19] showed a gradient of the glass transition in the vicinity of the particles for silica-filled elastomers. In the models proposed by Tsagaropoulos and Eisenberg[7,8] for polymer nanocomposites, the interfacial regions above certain content should exhibit their own glass transition at a temperature, which is considerably higher than that of the polymer. They observed two glass transitions for PVAc through dynamic mechanical analysis and interpreted the results with a three-layer model. However, the second transition observed by Tsagaropoulos and Eisenberg was suggested to be corresponding to the formation of a macroscopic "gel" by Salaniwal et al.[20] and be ascribed to the terminal relaxation process (chain diffusion) of un-cross-linked polymer suppressed by interaction with particles according to Robertson and Roland.[5] The interface of ultrathin polymer films on silicon oxide substrates has some similarity with that of the polymer/silica nanocomposites. In the early studies, the glass transition of the thin polymer films on silicon oxide showed an increase with decreasing film thickness.[21−23] This reveals that the interfacial regions in the polymer/silica nanocomposites have possibility to show a higher T_g. A second relaxation, ascribed to a surface layer of polymer with slower dynamics above the intrinsic glass transition in the tan δ spectra, was found by Arrighi and co-workers[24] when they studied the isochronal relaxation behavior of styrene−butadiene rubber containing silica nanofiller.

Computer simulations on the relaxation dynamics of materials under confinement effects have also been extensively studied.[25−29] Molecular dynamics simulation of a polymer melt with a nanoparticle by Starr et al.[28] showed that the glass transition temperature of the melt could be shifted to either higher or lower temperatures by tuning the interactions between polymer and nanoparticle. And for very thick bound polymer, a disparity in time scales between the inner and outer layers could lead to the presence of two (or more) detectable glass transitions. The results of molecular dynamics simulation for polymer nanocomposites studied by Brown et al.[29] showed that evidence for chain immobilization is less obvious in their model. But they also suggested that the "thickness" of the interphase is sensitive to the strength of the polymer−nanoparticle interaction.

Here we show and analyze the tan δ curves of PVA nanocomposites with various silica contents. A two-layer model is introduced, and the structure of the interfacial layer is discussed to interpret the results observed. PVA and silica sol were selected for this experiment for their strong interactions and the interfacial binding force. The interactions and the force could be strengthened via in-situ polymerization for the formation of chemical bonds.[30] It is noteworthy that silica sols obtained by the sol−gel

*Corresponding author. E-mail: pcui@issp.ac.cn.

 Published on Web 12/28/2009

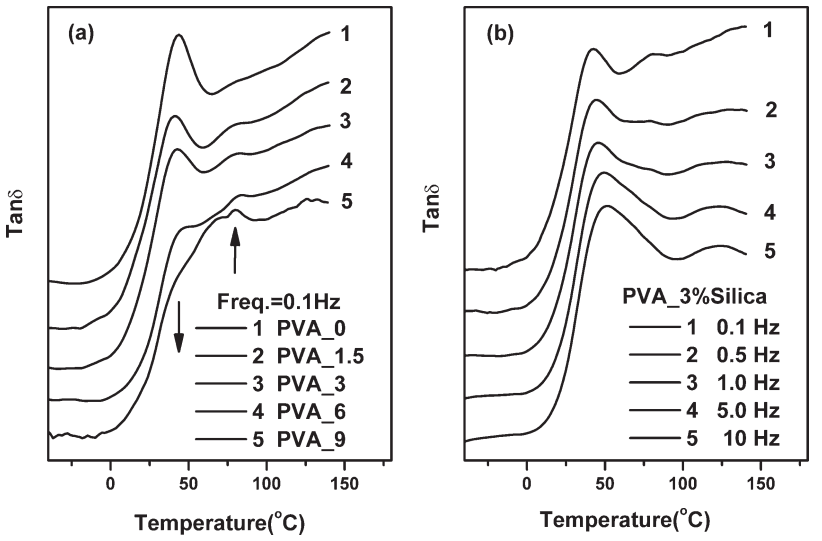

Figure 1. Tan δ vs temperature curves of (a) the pure PVA and the PVA/silica nanocomposites at 0.1 Hz and (b) the composite with 3 wt % silica content at different frequency.

process offer a versatile reactive surface easily forming Si−O−C bonds with organic molecules in some special situations. Moreover, the residual silanol groups in silica sols could act as centers of adsorption of molecules and form hydrogen bonds with hydroxyl groups in PVA.

Experimental Section

Vinyl acetate (VAc) was obtained from Runjie Chemicals (Shanghai, China). Methanol and ethyl alcohol absolute were purchased from Sinopharm Chemical Reagent Co., Ltd. Tetraethoxysilane (TEOS) was bought from Shanghai First Reagent Plant (Shanghai, China) and was used without further purification. Azodiisobutyronitrile (AIBN) was purchased from Shanghai Fourth Reagent Plant (Shanghai, China) and was purified by recrystallization into 95% ethanol.

Silica sol was prepared through sol−gel reaction involving hydrolysis and polycondensation of TEOS by using ethanol as main solvent. First, 0.15 mol of TEOS, 150 mL of ethanol, and 12 mL of deionized water were mixed in a flask with a reflux condenser under continuous stirring; 1 mL of ammonia was added to catalyze the hydrolysis. The solution was heated to 63 °C for 3 h and then up to 68 °C for half an hour in order to complete conversion of TEOS to silica. And then, the sol was concentrated to different silica weight fractions. The diameter of the silica particles is ca. 20 nm.

PVAc/silica nanocomposites were synthesized via an in-situ free radical polymerization with vinyl acetate as monomer and AIBN as initiator. And then, PVA/silica nanocomposites were obtained by direct alcoholysis of PVAc/silica nanocomposites with NaOH/methanol solution. In a typical procedure for preparation of the nanocomposites, a three-necked round-bottom flask (100 mL) with a condenser was charged with 50 mL of VAc, 10 mL of silica/ethanol sol, and 0.2 g of AIBN. The mixture was stirred and heated to 62 °C for 3 h under a N_2 atmosphere and then heated up to 68 °C for half an hour to complete the reactions. The product of PVAc/silica composites was transferred to a 500 mL three-necked flask and dissolved in 170 mL of methanol. After that, the mixture was heated to 32 °C, and 20 mL of 0.5 M $NaOH/CH_3OH$ solutions was added into the flask gradually in 1 min. The temperature was maintained for 2 h. And then, another 10 mL of 0.5 M $NaOH/CH_3OH$ solutions was added in the flask gradually and heated up to 60 °C for half an hour. The product was filtrated, washed with ethanol repeatedly, and dried in a vacuum oven at 50 °C for 24 h. By a similar procedure, a series of PVA/silica nanocomposites were prepared with the silica weight fractions of 1.5, 3.0, 6.0, and 9.0 wt %. The pure PVA and the composites were labeled as PVA_0, PVA_1.5, PVA_3, PVA_6, and PVA_9, respectively. The degree of polymerization of the pure PVA measured through viscometer method is ca. 600, and the degrees of alcoholysis for the samples measured via titration methods are all ca. 98%.

DMA experiments were performed using a Perkin−Elmer Diamond DMA instrument in tension mode at the heating rate of 1 °C/min using a dry nitrogen atmosphere. Differential scanning calorimetry was performed on a Pyris Diamond DSC (Perkin-Elmer), and all measurements were made at a scan rate of 20 °C/min under continuous nitrogen gas flow. The samples were investigated from 5° to 40° by Philips X' Pert Pro MPD X-ray diffractometer, and the infrared spectra were obtained from a Nicolet Nexus Fourier transform infrared spectrometer.

Experimental Results

Results of Dynamical Mechanical Analysis. Figure 1a shows the tan δ vs temperature curves for pure PVA and PVA/silica nanocomposites with different silica contents at 0.1 Hz. There is a peak with a maximum at ca. 43 °C corresponding to the glass transition of pure PVA. The relatively intensity of the peak decreases with the increase of the silica content, and the peak disappears in the PVA_9. The curve of the PVA_9 sample exhibits a broadening glass transition. This demonstrates that the chain segments participated in this relaxation for the composites decrease with the increase of the silica content.[7,24] It is interesting that there is another peak located at ca. 83 °C for all the composites, and this peak does not exist in the pure PVA curve. The relatively intensity of the peak increases with increasing silica content, which is quite different from the change of the peak due to glass transition for the PVA matrix. This phenomenon suggests that the second peak is probably associated with motions of the PVA chains confined by the silica particle surfaces. Figure 1b shows the tan δ versus temperature curves for PVA_3 at different frequencies. The peak due to glass transition for PVA matrix shifts to higher temperature with the increase of frequency for strain lag of the sample. It can be also found that relatively intensity of the second peak has a decrease at the frequency of 0.5 Hz and disappears at the frequency above 1.0 Hz.

For polymer/inorganic nanocomposites, segmental relaxation times where close to the filler surface are significantly longer than those of the unfilled polymer.[24] The temperature

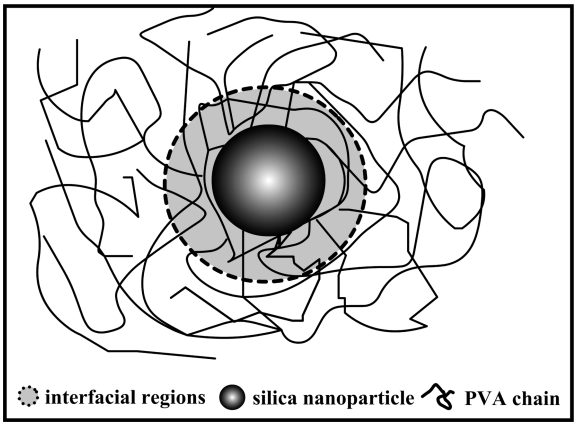

Figure 2. Two-layer schematic model of the PVA nanocomposite with silica nanoparticles (with PVA molecules spanning the two layers).

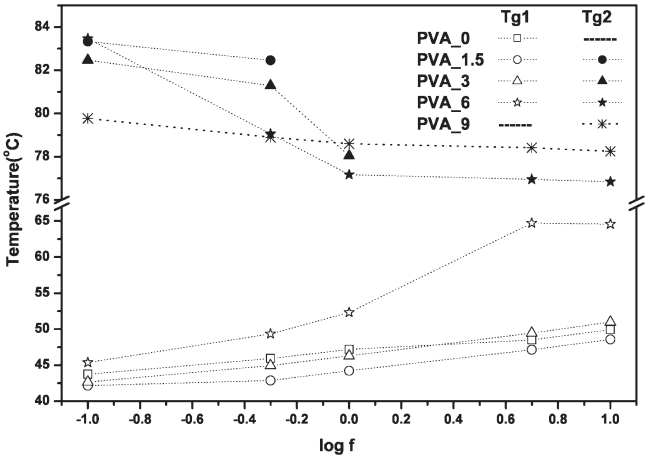

Figure 3. Temperature for the tan δ peak positions (T_{g1} and T_{g2}) versus the logarithm of frequency.

of the peak position for the second relaxation, a little higher than that of the PVA matrix, suggests that it is due to the glass transition of the interfacial layer constrained by the surface of silica nanoparticle. It is supposed that nanoparticles were well dispersed in PVA matrix; the results could be well in agreement with simple two-layer model (intrinsic and interfacial regions of PVA), with similarity to the model suggested by Park and McKenna used in polymer solutions constrained by nanometer scale pores.[11] Figure 2 shows the schematic structural model of the PVA nanocomposite with silica nanoparticles. It is considered that the PVA matrix exhibits the first T_g and the interfacial layers around silica nanoparticles exhibit the second.

Figure 3 shows the frequency dependence of the temperature for the tan δ peak positions. There is something interesting to notice from the data. The peak due to glass transition for PVA matrix moves to higher temperature with the increase of frequency for strain lag of the sample. However, the peak position of the second relaxation shifts to lower temperature with the increase of frequency. It is unclear why the second relaxation exhibits such behavior. In the model proposed by Park and McKenna,[11] which studied the effects of size and confinement of polymer solutions, PS chains could span two layers for their molecular size is big enough. Therefore, in two-layer model for the polymer nanocomposite, it is obvious that there are a lot of polymer chains spanning the two layers (as shown in Figure 2). Although the polymer chains tend to rotate in the direction

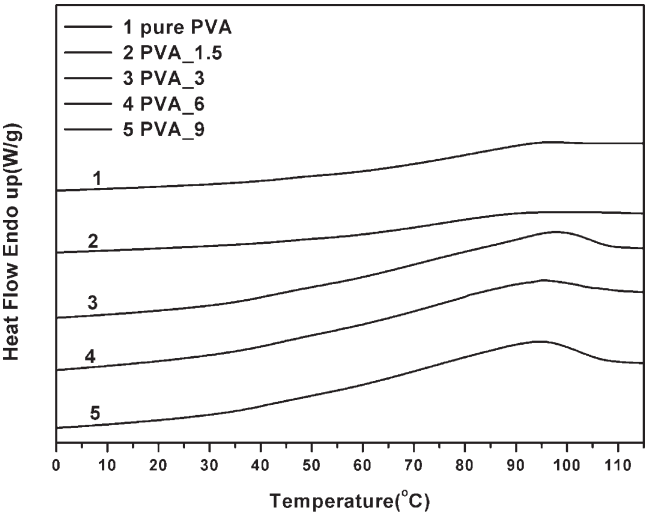

Figure 4. Glass transitions (DSC) of the pure PVA and its nanocomposites.

tangential to the nanoparticle surface due to confinement,[34] most of the molecules of the interfacial layer probably extend part of their segments to intrinsic amorphous layers. So there are many PVA molecules where one part of the molecule belongs to the intrinsic amorphous region and the other part belongs to the interfacial layer. Compared with those at high frequencies, polymer chains in the intrinsic layers have a relatively longer time to relax at low frequencies. In those molecules spanning two layers, the segments of the intrinsic layers have less impact on their interfacial parts during the first relaxation at low frequencies. But it is probably unavoidable that the intrinsic segments of the spanned molecules have a "drag effect" on the interfacial part during the dynamic measurement. And the effects of drag among the spanned molecules increase with the increase of frequency and result in the second relaxation ahead of time. It is considered that this is the possible reason for the temperature of the second peak position declining with the increasing frequencies.

Differential Scanning Calorimetry Studies. The glass transition was also obtained through DSC at a scan rate of 20 °C/min. Since the sensitivity of DSC is lower than that of DMA, the double glass transitions were not found in DSC curves. According to Wunderlich's work,[35] if the glass transition of the rigid amorphous fraction is approximately equal to the glass transition of mobile amorphous part, the DSC curve should indicate a broadening of the glass transition. Profiles in Figure 4 show the DSC glass transitions for the samples. The beginning of the glass transition for all the samples is seen at ca. 20 °C. The transition of the pure PVA looks complete at ca. 100 °C. The difference of temperature between the beginning and the end (ΔT) of glass transition is ca. 80 °C. However, the glass transition for PVA_1.5 is a little broader than that of the pure PVA. The glass transition for the other composites ranges from ca. 20 to 110 °C, and the ΔT is ca. 90 °C. That is, the addition of the silica nanoparticles broadens the glass transition in a nonisothermal scan through DSC.

Figure 5 presents the endothermic peaks of DSC profiles corresponding to the melting of PVA crystallites for pure PVA and its composites. The results for the samples are listed in Table 1. The melting points of the PVA_1.5 and PVA_3 are close to that of the pure PVA, suggesting that these three samples have similar crystallite size. However, the melting point shifts to lower temperature for PVA_6 and PVA_9,

indicating that the crystallite size made an obvious decrease. This phenomenon suggests that the silica nanoparticle has low impact on crystallite size when silica content is low and obstructs the crystallization of the PVA when the silica content is high. The area of endothermic peak for pure PVA and its composites gradually became smaller with the increase of silica content, indicating that the crystallinity of the samples decreased with increasing silica content. That is to say, the low amount of silica nanoparticles would only decrease the degree of crystallinity, but the large amount of silica nanoparticles would obstruct the crystallization of the matrix and result in a decrease in both crystallinity and crystallite size.

X-ray Diffraction Studies. Figure 6 shows the XRD curves for pure PVA and the composites. The peaks around $2\theta = 19.5°$ and 22.7° correspond to the mixture of (101) and ($10\bar{1}$) planes of the PVA crystals and (200) crystalline reflections,[36,37] respectively. The intensity of the peak at $2\theta = 19.5°$ decreases with increasing silica content in the PVA matrix. The degrees of crystallinity for PVA (X_c) were calculated using the method of crystalline and amorphous peak areas.[37] In order to get rid of the contributions of nanoparticles for polymer nanocomposites, the degree of crystallinity for the composites should be still revised by the equation

$$X_{cx} = X_c/(1-x) \quad (1)$$

where X_{cx} is the degree of crystallinity for the composite taking out the contribution of nanoparticle content and x is the weight fraction of the nanoparticles.

The values of $X_{c\text{-}XRD}$ are listed in Table 1. The data indicate that the degree of crystallinity for the composite declines gradually with increasing silica content. Many results had suggested that the restriction of chain mobility influenced by nanoparticles did not extend throughout the polymer matrix. Only the chains within several nanometers on the filler surface have this affection.[6,24,38] It is considered that PVA chains of the immobilized layer around the silica nanoparticle could not participate in the crystallization for the restriction of the nanoparticle surface. Consequently, the formation of the amorphous bound layer is probably the reason that the crystallinity for the composite decreases with the increase of silica content.

Infrared Results. To further confirm the crystallinity of the PVA/silica nanocomposites, FTIR was used for this study. Figure 7 shows the infrared spectra for the pure PVA and the PVA/silica nanocomposites. The band of 1143 cm^{-1} was assigned to the C−C stretching vibration in the crystals[39] or the O−C−C symmetric stretching vibration. The absorbance of this band (A_{1143}) was considered to depend on the degree of crystallinity. Meanwhile, the band of 1093 cm^{-1} was assigned to the O−C−C antisymmetric stretching vibration.[40] This band was considered as the contribution of the intermolecular hydrogen bonds and the amorphous parts of PVA, and its absorbance (A_{1093}) was independent of the degree of crystallinity. Figure 8 shows the dependency of (A_{1093}/A_{1143}) on the composites with different silica contents. The absorbance ratios (A_{1093}/A_{1143}) appear to increase steadily with the increase of silica content in the composites. It demonstrates that the degree of crystallinity for PVA decreases with the increase of silica content for the linear relationship between the absorbance ratio and an inverse the degree of crystallinity.[31] This trend is in good agreement with the DSC and XRD data.

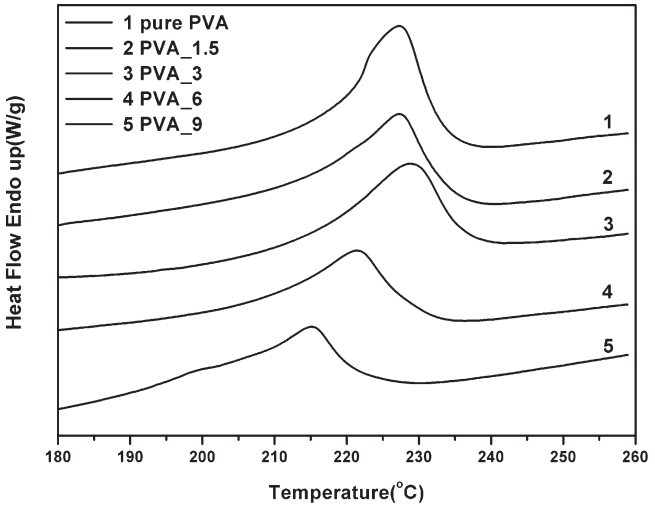

Figure 5. Melting curves of the pure PVA and its nanocomposites.

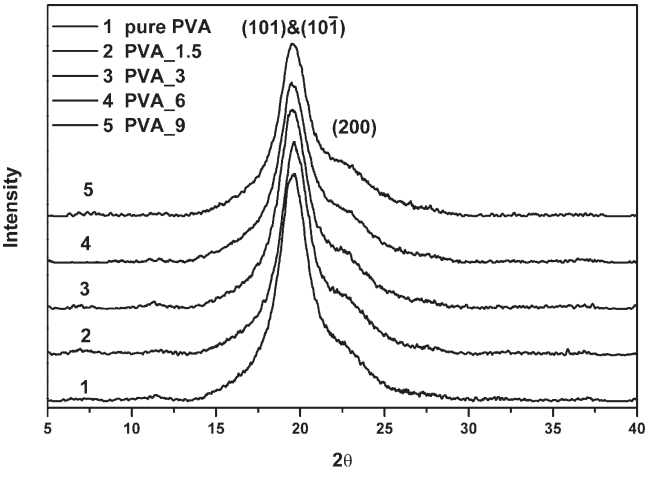

Figure 6. XRD patterns of the pure PVA and the PVA/silica nanocomposites.

Table 1. Silica Content by Volume, Mean Distance between Neighboring Nanoparticles D, the First Glass Transition T_{g1}, the Second Glass Transition T_{g2}, the Degree of Crystallinity $X_{c\text{-}XRD}$, Calculated Thickness L of the Immobilized Layer around the Silica Particles, and Parameters from DSC Curves for the Samples

			DMA data				DSC data			
sample	vol %	D^a (nm)	T_{g1}/°C	T_{g2}/°C	$X_{c\text{-}XRD}$	L^a (nm)	T_m/°C	ΔH/J/g	$X_{c\text{-}DSC}{}^a$	ΔT^a/°C
PVA_0	0		44		0.523		227	84.6	0.610	~80
PVA_1.5	0.9	58	42	83	0.488	10.1	227	73.2	0.528	~85
PVA_3	1.8	42	43	82	0.461	9.9	228	63.9	0.461	~90
PVA_6	3.6	29	45	83	0.451	7.1	221	60.7	0.438	~90
PVA_9	5.5	22		80	0.432	6.3	215	52.1	0.376	~90

[a] The data used for these calculations are a mass density for PVA amorphous region[31] of 1.269 and 2.2 g/cm^3 for the silica nanoparticles.[32] The diameter of the silica nanoparticle used here is 20 nm. The crystallinity for the PVA through DSC was calculated using the enthalpy of 138.6 J/g for a theoretical 100% crystalline PVA.[33] ΔT is difference of temperature between the beginning and the end of the glass transition for DSC curves.

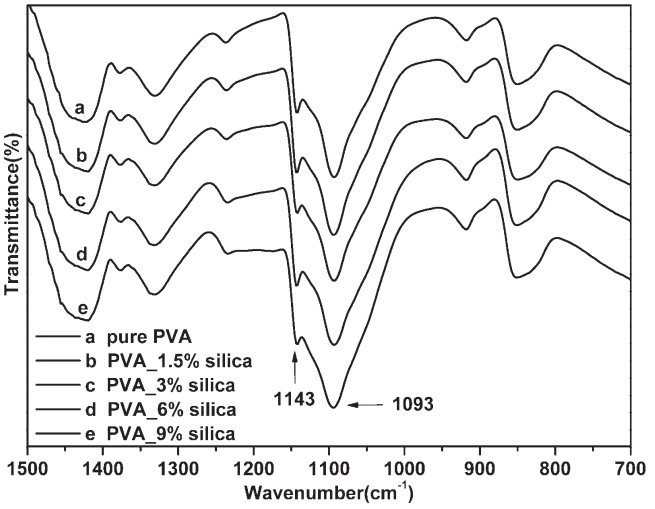

Figure 7. FTIR spectra of the pure PVA and the PVA/silica nanocomposites.

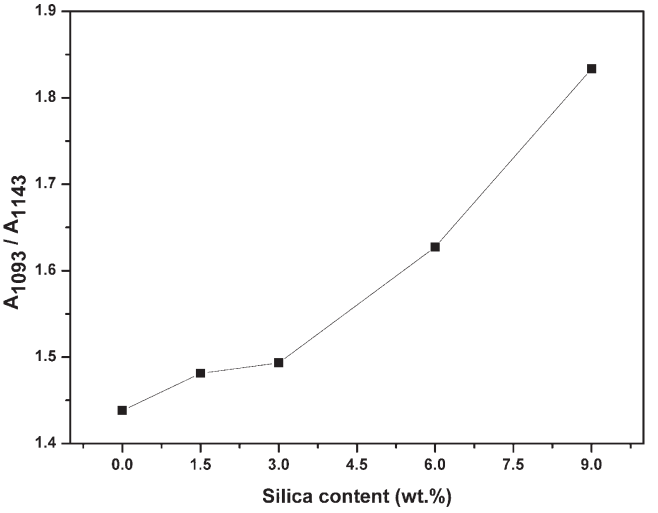

Figure 8. Values of A_{1093}/A_{1143} against silica content for pure PVA and the nanocomposites.

Thickness of the Interfacial Immobilized Layer. It is supposed that the impact of the nanoparticle surface on PVA chains only extends within several nanometers on the filler surface; the interfacial layer does not crystallize (as was taken also by Fragiadakis et al.[38] and Aranguren[41] for similar calculations), and nanoparticles could be well dispersed in polymer matrix. From the XRD and FTIR data, it was concluded that the degree of crystallinity of the composites decreased with the increase of silica content for the formation of the amorphous bound layer around the silica surface. According to the assumptions, the crystallized proportion of PVA with the exception of the interfacial regions in the composites could be taken as equality to that of the pure PVA. The nanoparticles could be approximately viewed as spheres, and the layer around the particle is considered as a spherical shell. Then, the mean thickness of the amorphous layer around the silica particle could be calculated by the equation

$$L = \left[\sqrt[3]{1+\frac{\rho_s}{x\rho_a}\left(1-\frac{X_{cx}}{X_p}\right)}-1\right]\frac{d}{2} \qquad (2)$$

where L is the thickness of the immobilized amorphous layer, X_p is the degree of crystallinity for pure polymer, X_{cx} refers to the degree of crystallinity for the composite taking out the contribution of nanoparticle content, ρ_a is the density of the amorphous regions for polymer, x is the weight fraction of the nanoparticles in the composite, and ρ_s and d are the density and the diameter of the nanoparticle, respectively.

It is considered that different polymer nanocomposites should have various thicknesses of the bound layers. The thickness of the interfacial layer probably dominated by three factors: the structure of the polymer, the diameter of the nanoparticle, and the structure of the nanoparticle surface. So PVA and silica sol particles with the diameter of 20 nm indicate that the thickness of the layer should be an invariable value. From the eq 2, the thickness of the restricted amorphous layer could be counted out with some known parameters. The results calculated with $X_{c\text{-}XRD}$ for the series composites are listed in Table 1. The thickness of the layer calculated with $X_{c\text{-}DSC}$ has a similar trend. It indicates that PVA_1.5 and PVA_3 have the approximately same thick layer on the silica surface. It demonstrates that these two composites have similar structure, and one core−shell unit (including nanoparticle and the interfacial shell) probably has little impact on another. From these results, it is concluded that the thickness of the layer around the nanoparticles is probably ca. 10 nm. However, the thickness of the immobilized layer has a dramatic drop in PVA_6 and PVA_9. The thickness of the layer for PVA_6 and PVA_9 decreases continuously to 7.1 and 6.3 nm, respectively. It indicates that the thickness of the interfacial layers decreases with the increase of silica content while the silica content is high. Since the thickness of the layer calculated by the eq 2 is an average value, the decrease of the thickness of the layer is corresponding to the reduction of the mean volume of one interfacial shell in the composites. For the composites in low silica content, the core−shell units could be well dispersed in the PVA matrix, and the space between two random ones is distant enough to avoid affecting each other. However, the mean distance of the neighboring nanoparticles decreases with the increase of silica content. The volume fractions and the mean distance between two random neighboring nanoparticles for the composites are listed in Table 1. It could be found that the mean distances between two neighboring particles are ca. 29 nm in PVA_6 and ca. 22 nm in PVA_9. Since the thickness of the interfacial layer is about 10 nm, the mean distance between the interfacial layers from neighboring core−shell units is only about several nanometers even though the nanoparticles dispersed ideally in the PVA matrix. Moreover, the affection of crystalline region could not be neglected for PVA is a kind of semicrystalline polymer. In the in-situ polymerization, the silica nanoparticles were well dispersed in the monomer before polymerization. Polymer/inorganic nanocomposites prepared by this effective technique could avoid the nanoparticles agglomerating at some extent. It is supposed that the nanoparticles were well dispersed in the PVA matrix; the simplified schematic model for the composite of Figure 9 is proposed.

Discussion

According to the process of preparation, the behavior of crystallization of PVA occurred after the dispersions of nanoparticles. The interfacial layer around the nanoparticles could not take part in the crystallization of the PVA matrix due to the confinement of the nanoparticle surface. Therefore, during the process of crystallization, the crystallizing behavior has little influence on the thickness of the interfacial layer in low silica

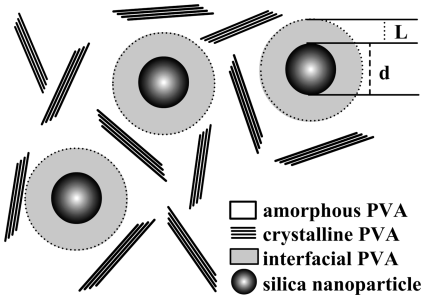

Figure 9. Simplified schematic model of the PVA nanocomposite with silica nanoparticles.

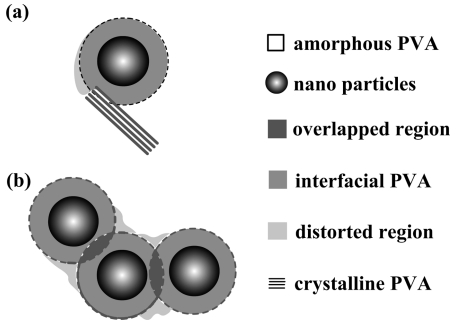

Figure 10. Schematic model of the interfacial layers affected by (a) crystalline region and (b) intershells in the PVA nanocomposite.

content composites for the mean distance between neighboring particles is distant enough. However, the mean distance of the neighboring particles decreases with the increase of silica content. Some crystals would probably intrude into the interfacial layers and push parts of the layer out of the interfacial region, as shown in Figure 10a. The parts of interfacial layer pushed out by crystals are some kind of distorted regions, which released from the silica surface confinement because they are far away from the silica surface. And then, these distorted regions become intrinsic amorphous regions (participate in the first glass transition). The interfacial PVA got out of the confinement of silica surface would decrease the volume of the interfacial layer. This is probably one reason for the reduction of the thickness of the interfacial layer for the high silica content composites.

Moreover, the growth of the crystals also probably could push a nanoparticle approaching the neighboring one, and this would result in the overlap of the interfacial layers among different shells. With the increasing silica content, the mean distance among neighboring particles decreases, and the overlapped regions among intershells increase under the effect of the crystallization. Figure 10b shows the overlapped schematic model among intershells in the composites. When the overlap of two core−shell units happens, some distorted regions are released from the impact of the silica surface and become intrinsic amorphous regions. This would also result in the reduction of the mean volume for one interfacial shell and is probably another reason that the thickness of the interfacial layer decreases with increasing silica content in the composites. Actually, the interfacial layers partly overlapped are inevitable in the composites when the silica content is above a critical value.

In the two-layer model for the polymer nanocomposites, polymer was divided in two parts: the intrinsic and interfacial layers. The boundary of the two layers is far away from the nanoparticle surface about several nanometers. However, polymer chain attributed to the interfacial layer entirely is rare because the size of the chain is pretty long. Therefore, most of the interfacial polymer chains probably span the two layers. In other words, the interfacial layer in the nanocomposite is mainly made up of partial segments of different polymer chains, which were confined by the nanoparticle surface. Hereby, for those spanned polymer chains, the relaxation of the intrinsic segments probably has influence on the interfacial part for they belong to one polymer chain. Moreover, the entanglement among polymer molecules would also increase the "drag effect" during the dynamic measurement. And with the increase of frequency, this influence is considered to be enhanced and results in the two relaxations exhibited a trend to approach. Then, the first relaxation exhibits shifting to high temperature and conversely for the second one with the increase of frequency; that is, the value of ΔT_g (the difference of T_{g2} and T_{g1}) declines with the increase of frequency.

When the confinement and size effects of nanoparticle surface are strong enough in the polymer nanocomposites, the second glass transition would be detectable above one critical nanoparticle content by a certain instrument such as DMA. If the nanoparticle content is below this critical value, the impact of the interfacial regions should be negligible and the composite should only exhibit one glass transition due to mobility of the intrinsic amorphous regions. When the second relaxation is detectable, the relatively intensity of the second peak should increase steadily along with the increase of the nanoparticle content and that of the first peak should do conversely. The reason is that the chain segments participated in the first glass transition for the composites decrease with the increase of the silica content and exhibit reverse for the second. When the nanoparticle content is above another critical value (the mean distance of two neighboring nanoparticles is less than double thickness of the interfacial layer above this critical content), the first glass transition would be replaced by a broad peak and disappear at last. Then, only the second glass transition is present because the intrinsic amorphous regions are negligible. At this time, the interfacial layers would be overlapped in a great measure for the distance of two neighboring particles is less than double thickness of the interfacial layer. After that, the peak of the first glass transition would completely disappear with continuously increasing silica content. That is to say, with the increase of nanoparticle content (begin with 0%), the nanocomposites should show in sequence one glass transition (the first T_g), double glass transitions (the first T_g and second T_g coexist), and one glass transition (a broadening T_g and then the second T_g). This trend is in agreement with the results observed in our tan δ spectra.

At this time, the crystalline region is introduced into the discussion. Since the thickness of the layer is definite for certain polymer nanocomposite, the presence of crystals would increase the relative proportion between interfacial regions and intrinsic amorphous regions. Therefore, the above-mentioned critical values of the nanoparticle content would have an enormous drop compared with those absolutely amorphous polymer nanocomposites. Even though the mean distance of the neighboring nanoparticles is far more than double thickness of the interfacial layer, the overlap of the interfacial layers in a great measure has probably happened because of the affection of the crystalline regions. For instance, Arrighi et al. found the second relaxation in the tan δ spectra of SBR filled with up to 20 wt % silica nanoparticles. And the phenomenon is better seen in the composites with 50 wt % silica nanoparticles. In direct contrast, the intensity of the second relaxation increased and conversely for that of the first relaxation with the increase of the filler content.[24] This trend is in agreement with our results. However, PVA with 1.5 wt % silica content has exhibited the second relaxation and a broadening glass transition appears in the PVA filled with 9 wt % silica content. One possible reason is that the thickness of the interfacial layer in PVA/silica nanocomposite (~10 nm) is thicker than that of the SBR/silica system (~2 nm). And another reason

is that PVA is a semicrystalline polymer, and the presence of crystals increases the relative proportion between interfacial regions and intrinsic amorphous regions. These two reasons help the PVA/silica nanocomposites have the lower critical silica contents mentioned above. These results are well in agreement with the discussions.

Conclusion

PVA/silica nanocomposite samples were produced via in-situ polymerization. Double tan δ peaks found in DMA curves correspond to the glass transitions of PVA matrix and the interfacial immobilized layer on the silica surface for the effect of confinement, respectively. For PVA nanocomposites, the temperatures of the peak position for the two relaxations have a trend to approach with the increase of frequency. These phenomena are probably ascribed to the increase of T_{g1} for strain lag of the samples and the decrease of T_{g2} for the "drag effect" between the intrinsic and interfacial parts of those spanned PVA chains during the dynamic measurements. A broadening of the glass transition was found in DSC data for the nanocpmposites and the degree of crystallinity of the samples decreased with the increase of silica content. From the XRD and FTIR data, it was also concluded that the degree of crystallinity decreased with the increase of silica content. It was considered that the immobilized layer existed around the silica particles is amorphous, which results in the reductions of the degree of crystallinity for the composites. The thickness of the interfacial layer for PVA/silica nanocomposites is ca. 10 nm, and the layer would be overlapped among the intershells while silica content is above a critical value. With the increase of silica content, the distance of the internanoparticles decreases gradually. When the distance of the two nanoparticles decreases to several nanometers, which is below the double thickness of the interfacial layer, the confinement of the nanoparticle surface should extend to the whole polymer chains of the composite. At this time, the first relaxation would disappear, and only the second one is present in the tan δ spectra. The results were well interpreted with the schematic models.

Acknowledgment. This work was supported by National Supporting Project (2007BAE22B03).

References and Notes

(1) Kickelbick, G. *Prog. Polym. Sci.* **2003**, *28*, 83–114.
(2) Bandyopadhyay, A.; Sarkar, M. D.; Bhowmick, A. K. *J. Polym. Sci., Polym. Phys.* **2005**, *43*, 2399–2412.
(3) Luo, L.; Yu, S. H.; Qian, H. S.; Zhou, T. *J. Am. Chem. Soc.* **2005**, *127*, 2822–2823.
(4) Alcoutlabi, M.; McKenna, G. B. *J. Phys.: Condens. Matter* **2005**, *17*, R461–R524.
(5) Robertson, C. G.; Roland, C. M. *Rubber Chem. Technol.* **2008**, *81*, 506–522.
(6) Sargsyan, A.; Tonoyan, A.; Davtyan, S.; Schick, C. *Eur. Polym. J.* **2007**, *43*, 3113–3127.
(7) Tsagaropoulos, G.; Eisenberg, A. *Macromolecules* **1995**, *28*, 396–398.
(8) Tsagaropoulos, G.; Eisenberg, A. *Macromolecules* **1995**, *28*, 6067–6077.
(9) O'Brien, J.; Cashell, E.; Wardell, G. E.; McBrierty, V. J. *Macromolecules* **1976**, *9*, 653–660.
(10) Yao, X.; Tian, X.; Xie, D.; Zhang, X.; Zheng, K.; Xu, J.; Zhang, G.; Cui, P. *Polymer* **2009**, *50*, 1251–1256.
(11) Park, J. Y.; McKenna, G. B. *Phys. Rev. B* **2000**, *61*, 6667–6676.
(12) Li, Q.; Simon, S. L. *Macromolecules* **2008**, *41*, 1310–1317.
(13) Gorbatschow, W.; Arndt, M.; Stannarius, R.; Kremer, F. *Europhys. Lett.* **1996**, *35*, 719–724.
(14) Huang, X.; Brittain, W. J. *Macromolecules* **2001**, *34*, 3255–3260.
(15) Tian, X. Y.; Zhang, X.; Liu, W. T.; Zheng, J.; Ruan, C. J.; Cui, P. *J. Macromol. Sci., Phys.* **2006**, *45*, 507–513.
(16) Ash, B. J.; Siegel, R. W.; Schadler, L. S. *J. Polym. Sci., Polym. Phys.* **2004**, *42*, 4371–4383.
(17) Bershtein, V. A.; Egorava, L. M.; Yakushev, P. N.; Pissis, P.; Sysel, P.; Brozova, L. *J. Polym. Sci., Polym. Phys.* **2002**, *40*, 1056–1069.
(18) Bogoslovov, R. B.; Roland, C. M.; Ellis, A. R.; Randall, A. M.; Robertson, C. G. *Macromolecules* **2008**, *41*, 1289–1296.
(19) Berriot, J.; Montes, H.; Lequeux, F.; Long, D.; Sotta, P. *Macromolecules* **2002**, *35*, 9756–9762.
(20) Salaniwal, S.; Kumar, S. K.; Douglas, J. F. *Phys. Rev. Lett.* **2002**, *89*, 258301-1–258301-4.
(21) Roth, C. B.; Dutcher, J. R. *J. Electroanal. Chem.* **2005**, *584*, 13–22.
(22) Keddie, J. L.; Jones, R. L.; Cory, R. A. *Faraday Discuss.* **1994**, *98*, 219–230.
(23) Zanten, J. H.; Wallance, W. E.; Wu, W. *Phys. Rev. E* **1996**, *53*, R2053–R2056.
(24) Arrighi, V.; McEwen, I. J.; Qian, H.; Serrano Prieto, M. B. *Polymer* **2003**, *44*, 6259–6266.
(25) Baschnagel, J.; Varnik, F. *J. Phys.: Condens. Matter* **2005**, *17*, R851–R953.
(26) Scheidler, P.; Kob, W.; Binder, K. *J. Phys. Chem. B* **2004**, *108*, 6673–6686.
(27) Scheidler, P.; Kob, W.; Binder, K. *Eur. Phys. J. E* **2003**, *12*, 5–9.
(28) Starr, F. W.; Schroder, T. B.; Glotzer, S. C. *Macromolecules* **2002**, *35*, 4481–4492.
(29) Brown, D.; Mele, P.; Marceau, S.; Alberola, N. D. *Macromolecules* **2003**, *36*, 1395–1406.
(30) Caregnato, P.; Le Roux, G. C.; Martire, D. O.; Gonzalez, M. C. *Langmuir* **2005**, *21*, 8001–8009.
(31) Sugiura, K.; Hashimoto, M.; Matsuzawa, S.; Yamaura, K. *J. Appl. Polym. Sci.* **2001**, *82*, 1291–1298.
(32) Landry, C. J. T.; Coltrain, B. K.; Landry, M. R.; Fitzgerald, J. J.; Long, V. K. *Macromolecules* **1993**, *26*, 3702–3712.
(33) Hassan, C. M.; Peppas, N. A. *Macromolecules* **2000**, *33*, 2472–2479.
(34) Picu, R. C.; Ozmusul, M. S. *J. Chem. Phys.* **2003**, *118*, 11239–11248.
(35) Wunderlich, B. *Prog. Polym. Sci.* **2003**, *28*, 383–450.
(36) Paranhos, C. M.; Soares, B. G.; Machado, J. C.; Windmoller, D.; Pessan, L. A. *Eur. Polym. J.* **2007**, *43*, 4882–4890.
(37) Minus, M. L.; Chae, H. G.; Kumar, S. *Polymer* **2006**, *47*, 3705–3710.
(38) Fragiadakis, D.; Pissis, P.; Bokobza, L. *Polymer* **2005**, *46*, 6001–6008.
(39) Tadokoro, H.; Seki, S.; Nitta, N. *J. Polym. Sci.* **1956**, *22*, 563–566.
(40) Liang, C. Y.; Pearson, F. G. *J. Polym. Sci.* **1959**, *35*, 303–307.
(41) Aranguren, M. I. *Polymer* **1998**, *39*, 4897–4903.